Active Disturbance Rejection Decoupling Control for Three-Degree-of-Freedom Six-Pole Active Magnetic Bearing Based on BP Neural Network

Shaoshuai Wang, Huangqiu Zhu, Mengyao Wu and Weiyu Zhang

School of Electrical and Information Engineering, Jiangsu University, Zhenjiang 212013, Jiangsu, China

26th International Conference on Magnet Technology
Poster ID :Mon-Mo-Po1.09-12
(Poster Session)

Background

Compared with the conventional mechanical bearings, magnetic bearings possess many promising advantages such as no mechanical contact, no lubrication, no wear, long life, high speed, and high precision, which have innovated the conventional supporting forms fundamentally. Due to these advantages, magnetic bearings have a broad prospect of application in high-speed machine tool spindles, flywheel systems, agile satellites, and so on. However, because of the strong nonlinearity and coupling effects, it is difficult to achieve the high precision and high speed operation of the magnetic bearings.active disturbance rejection control can handle these problems well.

Objectives

- Good performance of the three degrees of freedom six-pole active magnetic bearing (3-DOF 6-pole AMB) system while occurred the external disturbance.
- Outstanding decoupling performance between the variables in different directions.

3-DOF 6-pole AMB

A. Configuration and Working Principle

The configuration and magnetic circuits of the 3-DOF 6-pole AMB are shown in the figure. Due to the existence of the magnetic insulation aluminum ring, the axial control flux forms a loop among the axial stator, the axial air gap, the rotor, the radial air gap and radial stator. Radial control flux forms a loop among the radial stator, the radial air gap and the rotor.

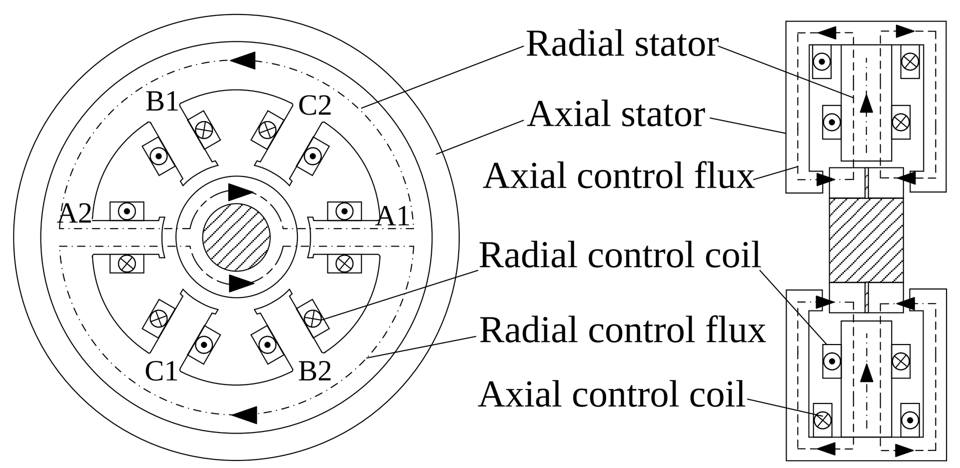

B. Suspension Force Mathematical Models

According to the equivalent magnetic circuit method and the configuration of the 3-DOF 6-pole AMB, radial and axial suspension forces mathematics models can respectively be obtained as:

$$\begin{cases} F_x = k_{ir}\cdot i_x + k_r\cdot x \\ F_y = k_{ir}\cdot i_y + k_r\cdot y \\ F_z = k_{iz}\cdot i_z + k_z\cdot z \end{cases} \quad k_{ir} = \frac{6\mu_0 S_a S_r N_2 N_a i_0}{(S_a+6S_r)\delta_0^2} \quad k_{iz} = -\frac{52 S_r^2 \mu_0 S_a N_a^2 i_0}{\delta_0^2 (S_a+6S_r)^2}$$

$$k_r = \frac{12\mu_0 S_a^2 S_r N_2 N_a i_0^2}{\delta_0^3 (S_a+6S_r)^2} \quad k_z = \frac{108\mu_0 S_a S_r^3 (N_a i_0)^2}{\delta_0^3 (S_a+6S_r)^3}$$

Supposing that the rotor has a small displacement z in the axial positive direction, x and y in the radial positive direction. Through the rotor's force analysis of the 3-DOF 6-pole AMB, we can derive the state equations of the system.

$$\begin{cases} \ddot{x} = \frac{3k_r}{2m}x_1 + \frac{k_{ir}}{m}u_1 - \frac{k_{ir}}{4m}u_2 - \frac{l_a J_z \Omega}{l J_d}x_5 \\ \ddot{y} = \frac{3k_r}{2m}x_2 - \frac{\sqrt{3}k_{ir}}{2m}u_1 - \frac{\sqrt{3}k_{ir}}{4m}u_2 + \frac{l_a J_z \Omega}{l J_d}x_5 \\ \ddot{z} = \frac{k_z}{m}x_3 + \frac{k_{iz}}{m}u_3 \end{cases}$$

ADRC-BP control algorithm

A. The structure of ADRC-BP

The ADRC-BP consists of two parts

- Conventional ADRC. It can directly control the controlled object, and its important component, ESO, has three adjustable parameters β_{01}, β_{02} and β_{03}.
- BP neural network. According to the running state of the system, the parameters of ESO are adjusted in real time, so that the controller can achieve optimal contrrol effect.

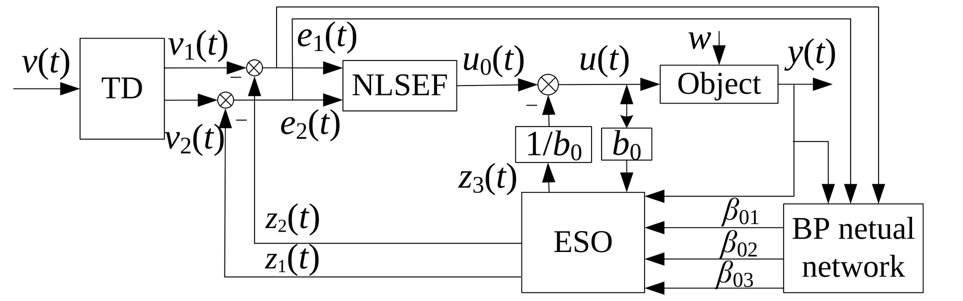

B. The structure BP neural network

The structure of BP neural network is a three-layer structure. Signal error e_1, differential signal error e_2, system output y and constant 1 are input nodes. The output nodes corresponds to the three adjustable parameters β_{01}, β_{02} and β_{03} of ESO.

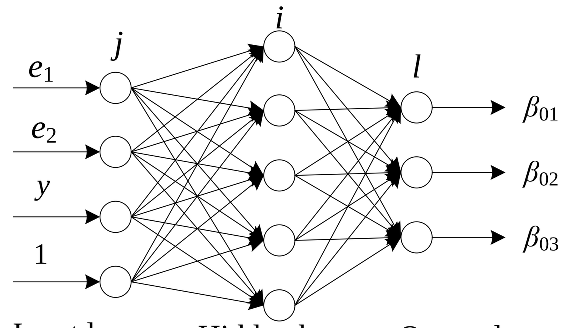

C. Decoupling control design of 6-pole AMB

The coupling between different degrees of freedom are regarded as the external disturbance of the system. Therefor, the 3-DOF 6-pole AMB system is converted into a multivariable, decoupled, and linear system. The decoupling control block diagram of the six-pole AMB based on ADRC-BP is shown in picture.

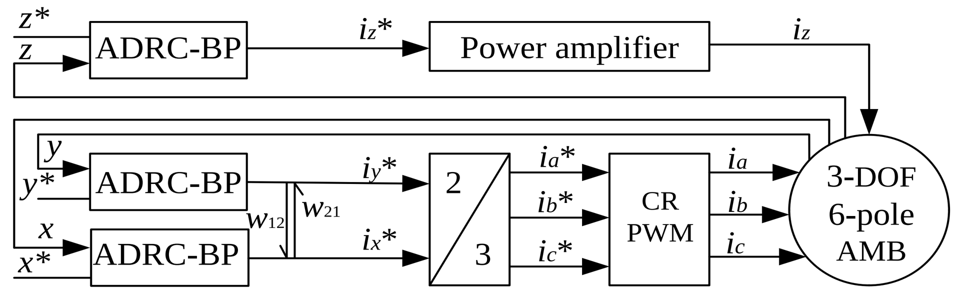

Simulation and experiment research

A. Simulation result

Assuming that the system is subjected to external disturbances with amplitudes of 150N varying according to sine. The figure on the right is the estimation curve of $z_3(t)$ to the disturbing force. As can be seen from the figure, when the system is subjected to 150N external disturbance force, the estimation error of ADRC-BP to the total disturbance is the smallest.

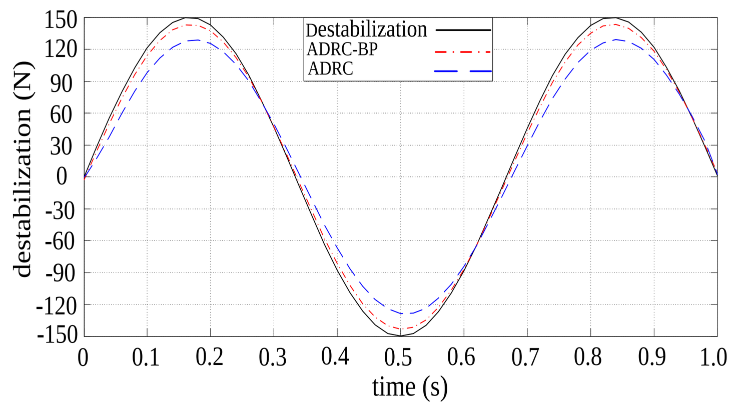

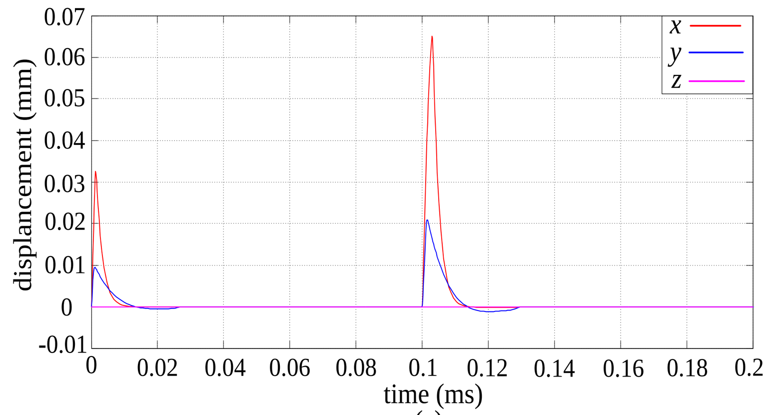

(a)

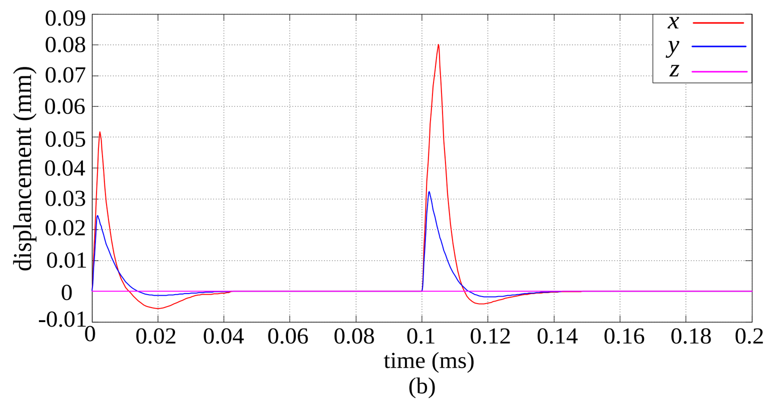

(b)

This figure on the left shows the disturbance response curves for 3-DOF 6-pole AMB under ADRC and ADRC-BP. When the rotor is stably suspended in the balance position, 50N and 150N instantaneous disturbances are applied to the x-direction of the rotor. As you can see from the figure, when the system is subjected to 150 N external disturbance force, the displacement in the x- and y-direction are the smallest. Therefore, the decoupling control effect and anti-interference ability of ADRC-BP are better than those of ADRC.

B. Experiment Research

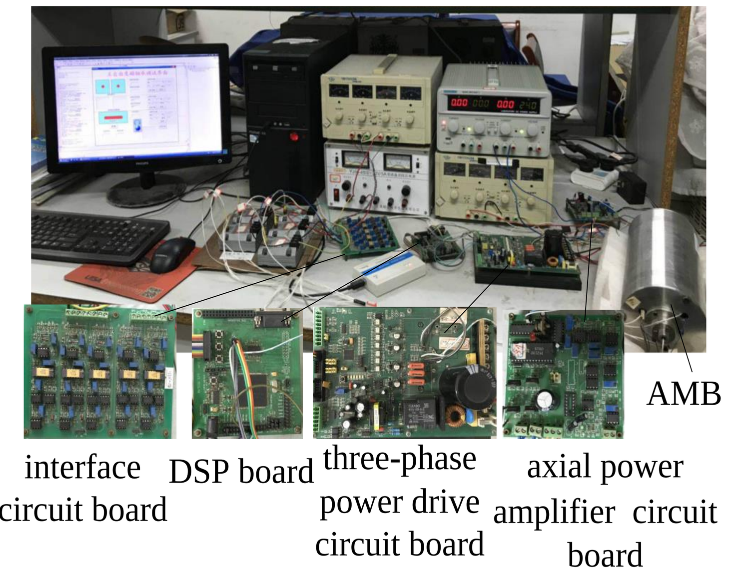

The length of air gap is designed to be 0.5 mm. However, to protect the experimental instruments, an auxiliary bearing was adopted to limit the rotor vibration to a 0.25 mm circle,which is placed on the end of the bearing so that it has no effect on the 3-DOF 6-pole AMB.

The variation with the external force of 100 N are shown in below figure. When the ADRC-BP controller is adopted, the variations in the x-direction are significantly reduced compared with that of ADRC. Consequently, the rotor returns to the original position faster using the ADRC-BP controller when the system is subjected to the external disturbance.

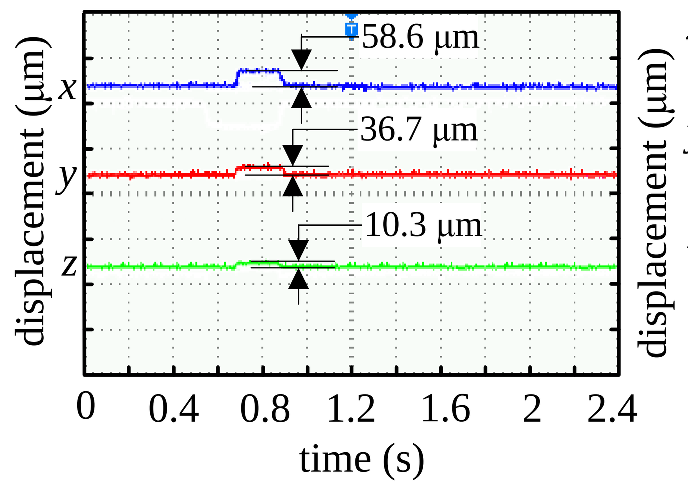

(a)

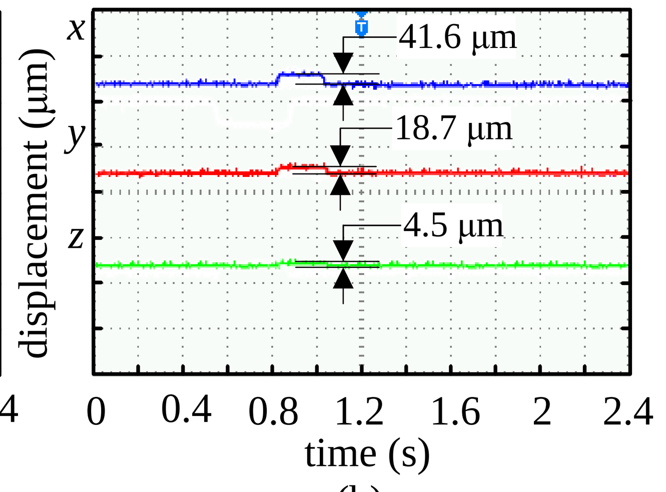

(b)

Conclusion

In this paper, by using the ADRC-BP, the 3-DOF 6-pole AMB system is converted into a multivariable, decoupled, and linear system. The effects of the configuration and suspension forces mathematical models are analyzed. The whole system of the 3-DOF 6-pole AMB in decoupling control based on ADRC-BP is designed. The simulation and experimental results indicate that, compared with the ADRC, the ADRC-BP can significantly suppress the interference and reduce the response time of the rotor. The above conclusions will be helpful to the high precision and high speed control of the AMB system.